Contribution from the Institut de Chimie Minérale et Analytique, Université de Lausanne, CH-1005 Lausanne, Switzerland, and the Laboratoire de Chimie de Coordination du CNRS, Université P. Sabatier, F-31030 Toulouse, France

Solution Structure and Dynamics of Five-Coordinate Nickel(II) Complexes with Trimethylphosphine: NiX_2L_3, $[NiXL_4]^+$, $[NiL_5]^{2+}$

PIERRE F. MEIER,[1a,b] ANDRÉ E. MERBACH,*[1a] MICHÈLE DARTIGUENAVE,*[1c] and YVES DARTIGUENAVE[1c]

Received September 7, 1978

The following complexes have been characterized in CH_2Cl_2 or $CHClF_2$ solutions between 114 and 295 K by $^{31}P\{^1H\}$ FT NMR and electronic spectroscopies: NiX_2L_3 (X = CN, Cl, Br, or I), $[NiXL_4]X$ (X = Cl, Br, or I), and $[NiL_5]^{2+}$ (with L = PMe_3). These complexes present a trigonal-bipyramidal geometry with the halide(s) in equatorial position and the cyanides in axial position. The intramolecular PMe_3 exchange in $[NiL_5](BF_4)_2$ ($\Delta G^* = 6.2$ kcal mol^{-1} at 130 K) and in $[NiXL_4]BF_4$ (X = Cl (6.6), Br (7.8), I (8.2) at 169 K) proceeds via a Berry pseudorotation. For $[NiXL_4]X$, the exchange rate is faster, proportional to the concentration of the ionic halide, and increases according to Cl < Br < I; an I_a mechanism with a 20-electron transition state is suggested. In $NiX_2(PMe_3)_3$ the energy barriers for the axial–equatorial phosphine exchange are higher (9.2–13.0 at 230 K); a D mechanism, with loss of an axial phosphine to form a four-coordinate intermediate, is proposed. The intermolecular exchange reactions $Ni(CN)_2L_3 + {}^*L \rightleftarrows Ni(CN)_2L_2{}^*L + L$ and $[NiXL_4]^+ + {}^*L \rightleftarrows [NiXL_3{}^*L]^+ + L$ (X = Cl or Br) are dissociative D.

Introduction

There have been many studies of substitution reactions in square-planar d^8 transition-metal complexes where five-coordinate trigonal-bipyramidal intermediates are postulated, but only recently, following the results of English, Jesson, and Meakin[2] on d^8 $[ML_5]^{n+}$ and $[MHL_4]^{m+}$, experimental information has been obtained about the nature of the five-coordinate intermediate, the role of intramolecular processes, and the determination of the rate of intermolecular ligand exchange vs. intramolecular rearrangement. These studies are important since they are necessary to get a valuable approach in the understanding of kinetics and mechanisms of organometallic and catalytic reactions.

To our knowledge, no systematic kinetic studies have been reported on the d^8 MX_2L_3 complexes. The only work on MX_2L_3 species is due to Hoffman and Caulton,[3] but the compounds studied were the d^6 $RuX_2(PPh_3)_3$ and $OsX_2(PPh_3)_3$ complexes. Compared to d^8 $[ML_5]^{2+}$ species, d^8 MX_3L_3 and $[MXL_4]^+$ complexes are less symmetrical molecules, with specific properties due to the relative electronic and steric requirements of the X and L ligands. Thus, they offer the opportunity to study the influence of X and L on the reactivity and to determine if the intra- and/or intermolecular rearrangement processes observed in d^8 $[ML_5]^{2+}$ molecules are still operating.

The nickel(II) complexes of trimethylphosphine represent a good system to be investigated, since the trans square-planar $NiX_2(PMe_3)_2$ (X = CN, Cl, or Br)[4] and $[NiX(PMe_3)_3]^+$ (X = Cl or Br),[5] the trigonal-bipyramidal *trans*-$Ni(CN)_2(PMe_3)_3$ (D_{3h}) and *cis*-$NiX_2(PMe_3)_3$ (C_{2v}),[4-8] and $[NiX(PMe_3)_4]BF_4$[9] (X = Cl, Br, or I) have been isolated and characterized.

The following two major equilibria (1) and (2) are observed in solution and are solvent, ligand, and temperature dependent.

$$NiX_2(PMe_3)_3 \underset{k_{-1}}{\overset{k_1}{\rightleftharpoons}} NiX_2(PMe_3)_2 + PMe_3 \qquad K_{inst} \qquad (1)$$

$$NiX_2(PMe_3)_3 + PMe_3 \underset{k_{-1}'}{\overset{k_1'}{\rightleftharpoons}} [NiX(PMe_3)_4]X \qquad K_{cat} \qquad (2)$$

Experimental Section

Chemicals. Trimethylphosphine[10] and the following complexes were synthesized according to known methods: $NiX_2(PMe_3)_2$ (X = CN, Cl, or Br),[4] $NiX_2(PMe_3)_3$ (X = CN, Cl, Br, or I),[4,7,8] $[NiX(PMe_3)_4](BF_4)$ (X = Cl, Br, or I).[9]

Solutions of $[NiX(PMe_3)_4]X$ (X = Cl, Br, or I) were prepared in situ in 10-mm NMR tubes by transferring PMe_3 to solutions of $NiX_2(PMe_3)_3$ in a 1:1 molar ratio in the vacuum line.

Dichloromethane (Fluka, analytical grade) was distilled twice from P_2O_5 and stored over 4-Å molecular sieves. Dichloromethane-d_2 (CEA, France) and chlorodifluoromethane (Freon 22, Du Pont) were used without further purification.

Electronic Spectroscopy. Electronic spectra were taken with a Cary 14 spectrophotometer (0.100-cm cells) equipped with a variable-temperature Oxford CF 100 Dewar (180–295 K). No correction has been done for the solvent contraction at 180 K.

NMR Spectroscopy. NMR Sample Preparation. The solid complexes were weighed in a nitrogen atmosphere glovebox (KSE) directly into 10-mm NMR tubes (Wilmad). The solvents were deoxygenated in an all-glass–Teflon vacuum line by the freeze–pump–thaw technique and vacuum distilled onto the solid samples. All tubes were sealed under vacuum and stored in liquid nitrogen to avoid formation of the "adduct" $PMe_3 \cdot CH_2Cl_2$.

NMR Measurements. Variable-temperature $^{31}P\{^1H\}$ FT NMR spectra were recorded at 36.43 MHz using a Bruker HX-90 spectrometer equipped with a B-SW 3PM pulser, a B-SV 3B proton noise decoupler, a B-ST 100/700 temperature regulating unit and a Nicolet BNC-12 data system. Some low-temperature (110–150 K) spectra were obtained at 24.28 MHz using a Bruker WP-60 spectrometer with multinuclei facilities. Field frequency stabilization was achieved on an internal ^2D signal at 21.14 kG and on an external ^{19}F signal at 14.09 kG. The temperature of the sample was measured before and after each spectrum by a method described elsewhere.[11]

Chemical Shift Referencing. As a ^{31}P chemical shift reference, we used pure PEt_3 in a capillary. Since the chemical shift of PEt_3 was temperature dependent (~0.03 ppm/K), we measured the chemical shift difference between PEt_3 and 62.5% H_3PO_4 (eutectic) as a function of temperature. All chemical shifts are reported with respect to 62.5% H_3PO_4, with downfield shifts considered positive.

Rate Constant Determination. In the case of intermolecular exchange in a two-site system, the following procedure was used. Chemical shifts of the complexed and free ligands (ν_C^0 and ν_F^0 in Hz) and line widths at half-height (W_C^0 and W_F^0 in Hz), in absence of ligand exchange, have been determined at low temperature where the reaction is frozen on the NMR time scale. To minimize the effect of instrumental broadening, the line width is given by

$$W = W^{measd} - W_{ref}^{measd} \qquad (I)$$

where W^{measd} is the actual width of the peak and W_{ref}^{measd} is the width of a nonexchanging reference, in our case PEt_3 in a capillary.

The values of τ_C^L and τ_F^L, the mean lifetime of the ligand in the complexed and free site, were obtained from the Bloch equations as modified by McConnell.[12]

In the slow-exchange region

$$1/\tau^L = \pi(W - W^0) \qquad (II)$$

$$1/\tau^L << (\pi/5)\Delta\nu_{CF}^0$$

Above coalescence, in the fast-exchange region

$$1/\tau_C^L = \frac{4\pi P_C P_F^2(\Delta\nu_{CF}^0)^2}{W - P_C W_C^0 - P_F W_F^0} \qquad (III)$$

$$1/\tau_C^L >> 2\pi\Delta\nu_{CF}^0$$

where $\Delta\nu_{CF}^0 = \nu_C^0 - \nu_F^0$ and where P_C and P_F are the relative population of the complexes and free sites ($P_C + P_F = 1$). τ_C^L and

0020-1669/79/1318-0610$01.00/0 © 1979 American Chemical Society

τ_F^L are related to the relative population by

$$P_C\tau_F^L = P_F\tau_C^L \qquad \text{(IV)}$$

In the case of intramolecular ligand exchange, we used the program PZDMCS of Meakin.[13] The intramolecular exchange rates were obtained by visual comparison of experimental and calculated spectra. The line shape calculations use density matrix methods coupled with group theoretical methods of permutational analysis and computer techniques for symmetry factoring.

The activation parameters were obtained from Arrhenius-like plots in which the best straight line has been determined by least-squares analysis, with the equation

$$\ln (k/T) = \ln (k_B/h) + \Delta S^*/R - \Delta H^*/RT \qquad \text{(V)}$$

where the symbols have their usual meaning.

Results

1. Solid-State Studies. Numerous structural studies on five-coordinate Ni(II) complexes appeared these last 10 years.[14] For compounds with monodentate ligands the trigonal-bipyramidal geometry is generally observed. However, one must remain cautious, since the energy difference between the trigonal bipyramid (TBP) and the square pyramid (SPY) is low as is shown by the crystal structures of $Ni(CN)_5^{3-}$ [5] and $Ni(CN)_2(phos)_3$ (phos = 5-methyl-5*H*-dibenzophosphole),[16] where the two isomers, SPY and distorted TBP, are reported in the same crystal. Moreover, very few regular TBP are reported. Guggenberger and Muetterties[17] have proposed a criterion based on interplanar angles of the coordination polyhedra to distinguish between the TBP and the SPY structures. Using this criterion, it can be shown that $NiBr_2(PMe_3)_3$[7,8] and $[NiBr(PMe_3)_4](BF_4)$[9] are best described as trigonal-bipyramidal complexes, distorted toward the square-pyramidal geometry along one of the $Ni-P_{eq}$ axes. $NiX_2(PMe_3)_3$ may exist as isomers trans (**1**), cis eq–eq (**2**),

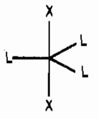

(1)

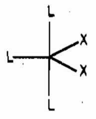

(2)

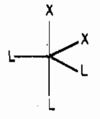

(3)

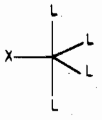

(4)

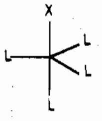

(5)

or cis ax–eq (**3**) and $[NiX(PMe_3)_4]^+$ as eq (**4**) or ax (**5**). The knowledge of the nature of the stereoisomer present in the solid state and in solution is important since it is related to the reactivity of the complexes.[18] The crystal structure determination of $NiBr_2(PMe_3)_3$ and $[NiBr(PMe_3)_4]BF_4$ has shown that in both complexes the bromine atoms are in equatorial positions (isomers **2** and **4**), results which agree with previous observations showing that, in Ni(II) and Co(II) five-coordinate complexes with phosphines, the halides prefer the equatorial positions.[9,19]

The crystal structure of $Ni(CN)_2(PMe_3)_3$ has not been reported, but the structures of analogous complexes, $Ni(CN)_2(PPhMe_2)_3$ and $Ni(CN)_2(PPh(OEt)_2)_3$, have been determined by Ibers et al.[20] as distorted TBP with the two CN ligands in axial position (isomer **1**). The similarity of the solid-state electronic and vibrational spectra[4] of $Ni(CN)_2(PMe_3)_3$ with those of the former complexes suggests a similar structure.

2. Solution Studies. Present knowledge of the solution behavior of Ni(II) five-coordinate complexes with monodentate phosphine or phosphite ligands is fractional. Since the work of Turco et al.,[21] who observed the higher stabilities of cyanide complexes compared to the halide one, the following complexes have been isolated: $NiX_2(PMe_3)_3$,[4] $NiX_2(PPhMe_2)_3$,[22] $NiX_2(PHPh_2)_3$,[23] $NiBr_2(PHEt_2)_3$,[24] $Ni(CN)_2(PR_3)_3$,[6,25] $NiX_2(P(OMe)_3)_3$,[26] $NiX_2(phos)_3$[16] (X = halide or CN), $[NiX(PHEt_2)_4](BPh_4)$,[24] $[NiBr(P(OMe)_3)_4](BF_4)$[27]. These complexes dissociate easily in solution, and excess of ligand is usually necessary to preserve the five-coordinate species. However, little has been done to study the nature of the species present in solution which was in part due to the lack of suitable spectroscopic probes.

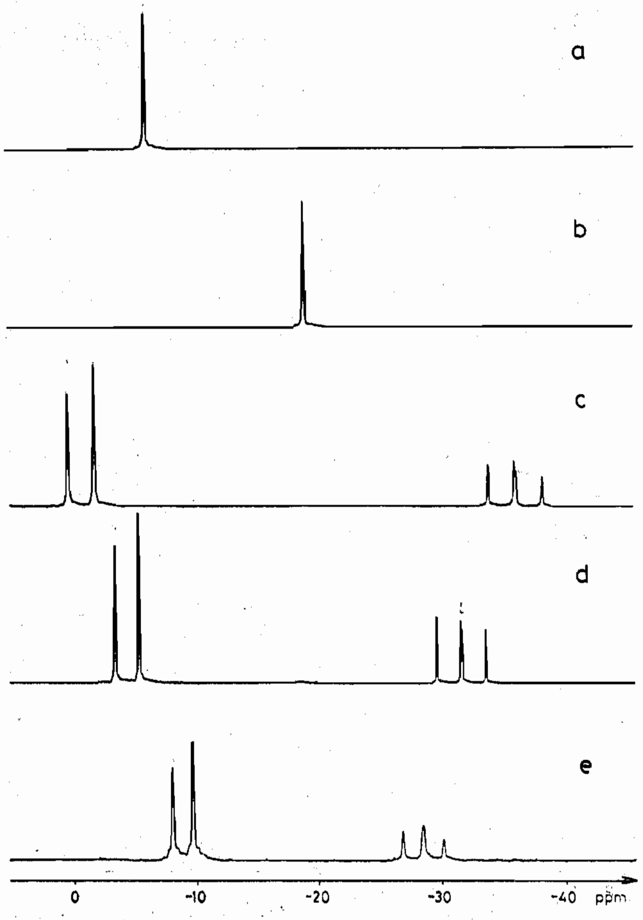

Figure 1. $^{31}P\{^1H\}$ FT NMR spectra at 36.43 MHz of (a) $Ni(CN)_2(PMe_3)_2$, 0.1 M at 198 K, (b) $Ni(CN)_2(PMe_3)_3$, 0.1 M at 198 K, (c) $NiCl_2(PMe_3)_3$, 0.05 M at 173 K, (d) $NiBr_2(PMe_2)_3$, 0.05 M at 183 K, and (e) $NiI_2(PMe_3)_3$ 0.05 M at 198 K in $CH_2Cl_2-CD_2Cl_2$ (1:1).

2.1 $Ni(CN)_2(PMe_3)_3$ Solutions. $Ni(CN)_2(PMe_3)_3$ has been assigned a trans trigonal-bipyramidal structure of D_{3h} symmetry on the basis of the vibrational and electronic spectroscopies and of magnetic, conductivity, and dipole moment determinations in solution.[4] The $^{31}P\{^1H\}$ NMR spectra in dichloromethane between 180 and 295 K show a sharp singlet ($\delta = -18.4$ at 198 K) indicating either that there are three equivalent PMe_3 ligands (A_3 spectrum) in the molcule or that the slow-exchange limit temperature is not reached and the molecule is still stereochemically nonrigid. The first assumption, i.e., an A_3 spectrum, is consistent with the expected D_{3h} TBP structure.

The instability constant K_{inst} describing the dissociation of $Ni(CN)_2(PMe_3)_3$ (eq 1) has been measured by electronic spectroscopy[4,6a] in dilute CH_2Cl_2 solutions (Table I). This dissociation is also observed at 198 K by ^{31}P NMR spectroscopy. Besides the $Ni(CN)_2(PMe_3)_3$ signal at −18.4 ppm, a weak singlet is resolved at $\delta = -5.7$, which is assigned to the square-planar $Ni(CN)_2(PMe_3)_2$ species (Figure 1). To confirm the attribution of the −5.7 ppm singlet to $Ni(CN)_2(PMe_3)_2$, we have isolated this species and measured its ^{31}P and ^1H NMR spectra, which agree well with the results previously reported (^1H NMR gives a pseudotriplet $X_nAA'X'_n$ pattern characteristic of a trans square-planar complex[6]). No new species is obtained when excess PMe_3 is added to a $Ni(CN)_2(PMe_3)_3$ solutions, since the 198 K ^{31}P NMR spectrum shows only the two singlets due to $Ni(CN)_2(PMe_3)_3$ and free PMe_3. This is consistent with the temperature de-

Table I. Equilibrium Constant K_{inst} (mol L^{-1}), Rate Constant k_1 (s^{-1}), Free Energy of Reaction $\Delta G°$ (kcal mol^{-1}), and Free Energy of Activation ΔG^* (kcal mol^{-1}) for the Reaction

$$\mathrm{Ni(CN)_2L_3} \underset{k_{-1}}{\overset{k_1}{\rightleftharpoons}} \mathrm{Ni(CN)_2L_2} + \mathrm{L} \qquad K_{\text{inst}} = k_1/k_{-1}$$

L	$10^4 \times K_{\text{inst}}$	$10^{-4}k_1$	$\Delta G°$	ΔG^*	T, K	solvent	ref
PMe_3	2.5	11.6[a]	+4.9	10.5[a]	298	CH_2Cl_2	6a
$PMe_2(OMe)$	0.4		+6.0		298	CH_2Cl_2	6a
$PMe(OMe)_2$	0.5		+5.8		298	CH_2Cl_2	6a
$P(OMe)_3$	1.7		+5.1		298	CH_2Cl_2	6a
$P(OEt)_3$	11.1	1.0	+4.0	12.0	298	CH_2Cl_2	6b
PEt_3	5260		+0.4		293	$C_2H_4Cl_2$	21
$PPh(Me)_2$	0.75	0.47	+5.6	12.4	298	CH_2Cl_2	6b
$PPh(Et)_2$	107		+2.6		293	$C_2H_4Cl_2$	21
$PPh(OEt)_2$	6.6	0.29	+4.3	12.7	298	CH_2Cl_2	6b
PPh_2Et	1950		+0.9		298	CH_2Cl_2	22
PPh_2Et	4166		+0.5		293	$C_2H_4Cl_2$	21
$PPh_2(OEt)$	560	2.9	+1.7	11.3	298	CH_2Cl_2	6b

[a] This work.

pendence of the electronic spectrum of $Ni(CN)_2(PMe_3)_3$ which showed nearly no difference with and without excess PMe_3 between 180 and 295 K.[4]

At 198 K, no intermolecular PMe_3 exchange is observed either between $Ni(CN)_2(PMe_3)_3$ and $Ni(CN)_2(PMe_3)_2$ or between $Ni(CN)_2(PMe_3)_3$ and free PMe_3. This exchange begins at higher temperature and above 300 K a single line is observed in both systems. This provides an opportunity to investigate the mechanism of intermolecular phosphine exchange. The two following reactions have been studied by variable-temperature ^{31}P NMR.

$$\mathrm{Ni(CN)_2(PMe_3)_3} + {}^*\mathrm{PMe_3} \rightleftharpoons \mathrm{Ni(CN)_2(PMe_3)_2({}^*PMe_3)} + \mathrm{PMe_3} \quad (3)$$

$$\mathrm{Ni(CN)_2(PMe_3)_3} + \mathrm{Ni(CN)_2({}^*PMe_3)_2} \rightleftharpoons \mathrm{Ni(CN)_2(PMe_3)_2} + \mathrm{Ni(CN)_2({}^*PMe_3)_2(PMe_3)} \quad (4)$$

If these two reactions occur through a *dissociative* D mechanism, the rate-determining step can be written as

$$\mathrm{Ni(CN)_2(PMe_3)_3} \xrightarrow{k_1} \mathrm{Ni(CN)_2(PMe_3)_2} + \mathrm{PMe_3} \quad (5)$$

and $\tau_{\mathrm{NiX_2L_3}}$, the mean lifetime of the $Ni(CN)_2(PMe_3)_3$ species, is related to the kinetic law by the expression

$$1/\tau_{\mathrm{NiX_2L_3}} = -\mathrm{d[NiX_2L_3]}/(\mathrm{[NiX_2L_3]d}t) = k_1 \quad (6)$$

where $\tau_{\mathrm{NiX_2L_3}}$ is related to the mean lifetime of the ligand in NiX_2L_3, $\tau_{\mathrm{NiX_2L_3}}{}^{\mathrm{L}} = \tau_{\mathrm{C}}{}^{\mathrm{L}}$, by relations 7 and 8 for the exchange reactions 3 and 4, respectively.

$$\tau_{\mathrm{NiX_2L_3}}{}^{\mathrm{L}} = 3\tau_{\mathrm{NiX_2L_3}} \quad (7)$$

$$\tau_{\mathrm{NiX_2L_3}}{}^{\mathrm{L}} = {}^3/_2\tau_{\mathrm{NiX_2L_3}} \quad (8)$$

If reaction 3 is controlled by an *associative* A mechanism, the rate-determining step will be

$$\mathrm{Ni(CN)_2(PMe_3)_3} + {}^*\mathrm{PMe_3} \xrightarrow{k_2} \{\mathrm{Ni(CN)_2(PMe_3)_3({}^*PMe_3)}\} \quad (9)$$

and $\tau_{\mathrm{NiX_2L_3}}$ will be related to the kinetic law by

$$1/\tau_{\mathrm{NiX_2L_3}} = k_2[\mathrm{L}] \quad (10)$$

and if reaction 4 is controlled by an associative mechanism we may write

$$\mathrm{Ni(CN)_2(PMe_3)_3} + \mathrm{Ni(CN)_2({}^*PMe_3)_2} \xrightarrow{k_2} \{\mathrm{(CN)_2Ni(PMe_3)_3({}^*PMe_3)_2Ni(CN)_2}\} \quad (11)$$

and the expression for $\tau_{\mathrm{NiX_2L_3}}$ will be

$$1/\tau_{\mathrm{NiX_2L_3}} = k_2[\mathrm{NiX_2L_2}] \quad (12)$$

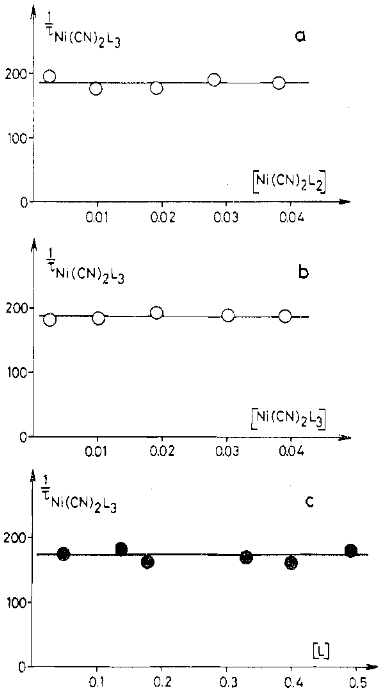

Figure 2. Determination of the rate law for the system $Ni(CN)_2L_2$–$Ni(CN)_2L_3$–L (L = PMe_3) in CH_2Cl_2–CD_2Cl_2 (1:1) at 237 K: (a) $[Ni(CN)_2L_3] = 9.1 \times 10^{-3}$ M; (b) $[Ni(CN)_2L_2] = 10.0 \times 10^{-3}$ M; (c) $[Ni(CN)_2L_3] = 10.0 \times 10^{-3}$ M.

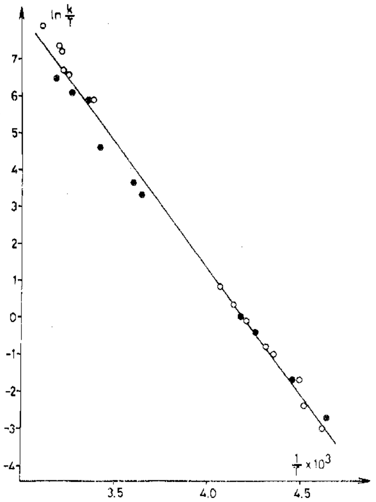

Figure 3. Arrhenius plot for the system $Ni(CN)_2L_2$–$Ni(CN)_2L_3$–L (L = PMe_3) in CH_2Cl_2–CD_2Cl_2 (1:1): (○) $Ni(CN)_2L_2$–$Ni(CN)_2L_3$ system, $[Ni(CN)_2L_2] = 0.025$ M, $[Ni(CN)_2L_3] = 0.03$ M; (●) $Ni(CN)_2L_3$–L system, $[Ni(CN)_2L_3] = 0.03$ M, [L] = 0.18 M.

The rate law has been determined at a fixed temperature by varying the concentrations of the different species. As shown in Figure 2, there is no dependency of $1/\tau_{\mathrm{NiX_2L_3}}$ on the free L, NiX_2L_2, and NiX_2L_3 concentrations. This indicates that the reaction is first order in $Ni(CN)_2(PMe_3)_3$ and zero order with respect to $Ni(CN)_2(PMe_3)_2$ and PMe_3. Equation 6 is used to determine k_1. Values of k_1 as a function of temperature are reported in Figure 3. From this Arrhenius-like plot of k_1, we determined the activation parameters for reactions 3 and 4. The activation parameters (Table II) are equal for both reactions within experimental error. The free energy of activation measured for the PMe_3 exchange is of the same order of magnitude as those previously reported for various phosphine, phosphite, and phosphonite exchanges on $Ni(CN)_2L_3$ (Table I). As shown by Grimes and Pearson,[6b] the cyanide exchange, much slower than the phosphine ex-

Table II. Activation Parameters ($L = PMe_3$)

process	ΔG^*, kcal mol^{-1}	ΔH^*, kcal mol^{-1}	ΔS^*, cal K^{-1} mol^{-1}
$Ni(CN)_2L_3$ + L intermolecular	11.3 ± 0.2^a	13.2 ± 0.5	$+10.1 \pm 2$
$Ni(CN)_2L_2$ + $Ni(CN)_2L_3$ intermolecular	11.4 ± 0.2^a	14.3 ± 0.5	$+12.6 \pm 2$
$NiCl_2L_3$ intramolecular	9.2 ± 0.2^a	11.5 ± 0.6	$+10.1 \pm 3$
$NiBr_2L_3$ intramolecular	10.5 ± 0.2^a	13.3 ± 0.9	$+12.5 \pm 4$
NiI_2L_3 intramolecular	13.0 ± 0.2^a	16.6 ± 1.0	$+15.7 \pm 4$
$[NiClL_4]BF_4$ intramolecular	6.6 ± 0.2^b		
$[NiBrL_4]BF_4$ intramolecular	7.8 ± 0.2^b		
$[NiIL_4]BF_4$ intramolecular	8.2 ± 0.2^b		
$[NiL_5](BF_4)_2$ intramolecular	6.2 ± 0.2^c		
$[NiClL_4]Cl$ + L intermolecular	8.4 ± 0.2^a	13.0 ± 1.2	$+20 \pm 6$
$[NiBrL_4]Br$ + L intermolecular	9.5 ± 0.2^a	11.3 ± 0.8	7.6 ± 4

[a] At 230 K in CH_2Cl_2–CD_2Cl_2 (1:1). [b] At 169 K in CH_2Cl_2–CD_2Cl_2 (1:1). [c] At 130 K in $CHClF_2$.

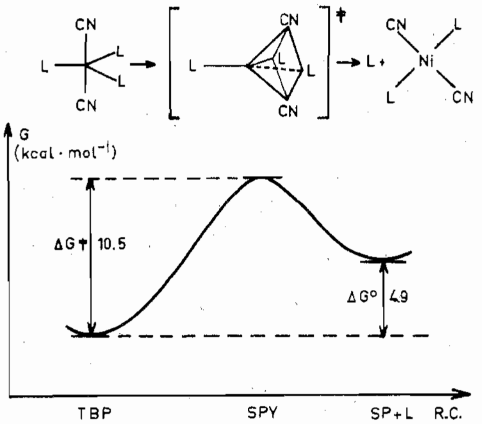

Figure 4. Schematic reaction coordinate for the ligand dissociation in $Ni(CN)_2L_3$ complexes. Numerical values are for $L = PMe_3$ at 298 K.

change, does not interfere with reactions 3 and 4. The positive entropy of activation and the first-order rate law indicate a dissociative D mechanism for the intermolecular phosphine exchange reaction. The intermediate is the square-planar $Ni(CN)_2(PMe_3)_2$. Schematic free energy change along the reaction coordinate is shown in Figure 4. This result is in agreement with the usual assumption that the ligand substitution in square-planar d^8 complexes occurs through intermediates of TBP geometry with the entering ligand in the equatorial plane. But here, the TBP species is the ground state and the square-planar species the intermediate.

2.2 $NiX_2(PMe_3)_3$ (X = Cl, Br, or I) Solutions without Excess PMe_3. The solution study of the $NiX_2(PMe_3)_3$ complexes presents a puzzling problem since tremendous variations of the electronic spectra have been observed as a function of the concentration of the complexes, the presence or not of excess PMe_3, the temperature, and the solvent. While in toluene (ϵ 2.5 at 298 K) only the molecular $NiX_2(PMe_3)_3$ species is observed, in dichloromethane (ϵ 9.1 at 293 K), various species are present.

As shown by electronic spectroscopy (Figure 5) at room temperature in dichloromethane, $NiX_2(PMe_3)_3$ dissociates according to reaction 1. The four-coordinate complexes $NiX_2(PMe_3)_2$ may be isolated from these solutions when X = Cl or Br as square-planar low-spin Ni(II) complexes. When X = I, no definite compound is obtained. We did not succeed in getting reproducible values of the equilibrium constants K_{inst} by electronic spectroscopy, due to the thermal and photochemical instability of these five-coordinate complexes in CH_2Cl_2 solutions at room temperature.

The temperature dependence of the electronic spectrum of $NiCl_2(PMe_3)_3$ is reported in Figure 6. Similar curves have been obtained for X = Br and X = I. It is apparent, from these spectra, that lowering the temperature increases the concentration of the five-coordinate species in solution. At 180 K, for a 10^{-2} M solution, no dissociation is detectable. These results are being confirmed by variable-temperature ^{31}P NMR.

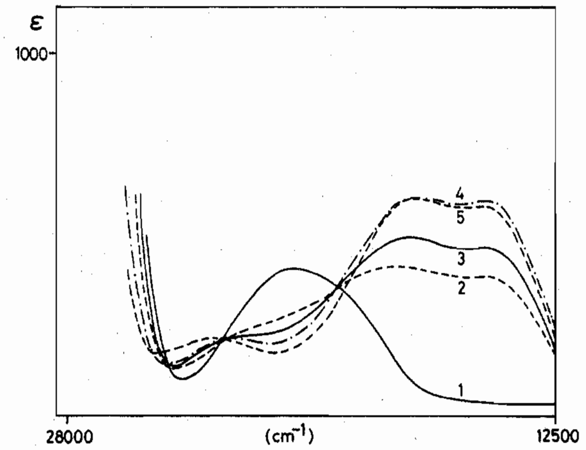

Figure 5. Electronic spectra of solutions of $NiCl_2(PMe_3)_2$ (C) and PMe_3 (L) in CH_2Cl_2 at room temperature: (1) [C] = 2.21×10^{-2} M; (2) [C] = 1.04×10^{-2} M, [L] = 1×10^{-2} M; (3) [C] = 1.34×10^{-2} M, [L] = 2×10^{-2} M; (4) [C] = 0.85×10^{-2} M, [L] = 3×10^{-2} M; (5) [C] = 0.89×10^{-2} M, [L] = 10×10^{-2} M.

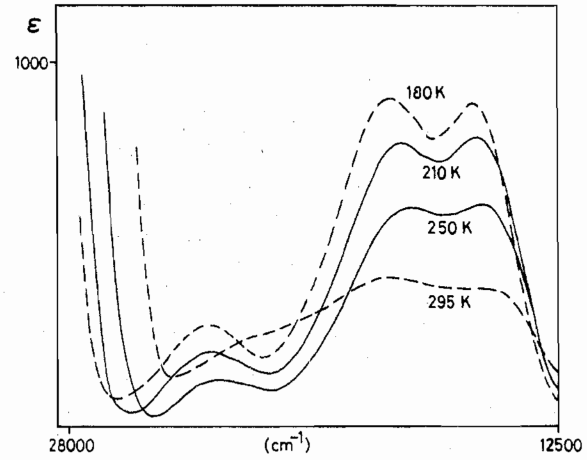

Figure 6. Temperature dependence (180–295 K) of the electronic spectrum of a solution of $NiCl_2(PMe_3)_3$ in CH_2Cl_2, $[NiCl_2(PMe_3)_3] = 10^{-2}$ M.

The five-coordinate complexes $NiX_2(PMe_3)_3$ are stereochemically nonrigid at ambient temperature on the NMR time scale but become stereochemically rigid at low temperature. The slow exchange limit spectra of 0.05 M solutions of $NiX_2(PMe_3)_3$ in dichloromethane are shown in Figure 1 and the NMR parameters in Table III. The exchanges are frozen at temperatures ranging from 173 K for X = Cl to 198 K for X = I. In these solutions, no other species are found at these temperatures at concentrations detectable by NMR. The ^{31}P NMR spectra are of the A_2B type with $J/\Delta\nu$ ranging from 6.2×10^{-2} for X = Cl to 8.4×10^{-2} for X = I. When the temperature is increased, the multiplets broaden, because of axial–equatorial ligand exchange, and collapse into a single line (Figure 7). This line sharpens by increasing the temperature and at still higher temperature (about 250 K for X = Cl and 270 K for X = Br) the line begins to broaden and shifts downfield, showing a new exchange process. English, Meakin, and Jesson[2] have observed the same phenomenon in their study of the mutual ligand exchange in the complex $[HNi(PEt_3)_4]^+$ in acetone, but no explanation was given. A

Table III. 36.43 MHz $^{31}P\{^1H\}$ FT NMR Data ($L = PMe_3$)[i]

product	geometry	$\delta_{P_{ax}}$[a]	$\delta_{P_{eq}}$[a]	J_{PP}[b]	T, K
$Ni(CN)_2L_2$	trans-SP		−5.7 s		198[c]
$NiCl_2L_2$	trans-SP		−20.4 s		183[c]
$NiBr_2L_2$	trans-SP		−19.2 s		183[c]
$[NiClL_3]BF_4$[h]	SP	−4.0[e]	−9.6[f]	85.6	180[c]
$[NiBrL_3]BF_4$[h]	SP	−1.3[e]	−11.1[f]	82.3	180[c]
$[NiL_4](BF_4)_2$[h]	SP		−17.3 s		123[d]
$Ni(CN)_2L_3$	trans-TBP		−18.4 s		198[c]
$NiCl_2L_3$	cis-TBP	−0.4 d	−35.0 t	79.0	173.1[c]
$NiBr_2L_3$	cis-TBP	−3.7 d	−30.4 t	72.0	173.1[c]
NiI_2L_3	cis-TBP	−8.7 d	−28.0 t	60.0	173.1[c]
$[NiClL_4]Cl$	Cl_{eq}-TBP	+1.5 t	−28.6 t	79.0	114[d]
$[NiClL_4]BF_4$	Cl_{eq}-TBP	+1.0 t	−28.8 t	82.5	163[c]
$[NiBrL_4]Br$	Br_{eq}-TBP	−15.7[g]			114[d]
$[NiBrL_4]BF_4$	Br_{eq}-TBP	−2.6 t	−29.2 t	79.0	163[c]
$[NiIL_4]I$	I_{eq}-TBP	−18.4[g]			114[d]
$[NiIL_4]BF_4$	I_{eq}-TBP	−5.2 t	−29.2 t	76.5	163[c]
$[NiL_5](BF_4)_2$	TBP	+0.9 q	−32.7 t	70.6	114[d]

[a] In ppm. [b] In Hz. [c] In CH_2Cl_2-CD_2Cl_2 (1:1). [d] In $CHClF_2$. [e] Phosphorus trans to the halogen. [f] Phosphorus cis to the halogen. [g] Broad signal. [h] Reference 39. [i] Chemical shift of free PMe_3 = −61.2 ppm at 173 K.

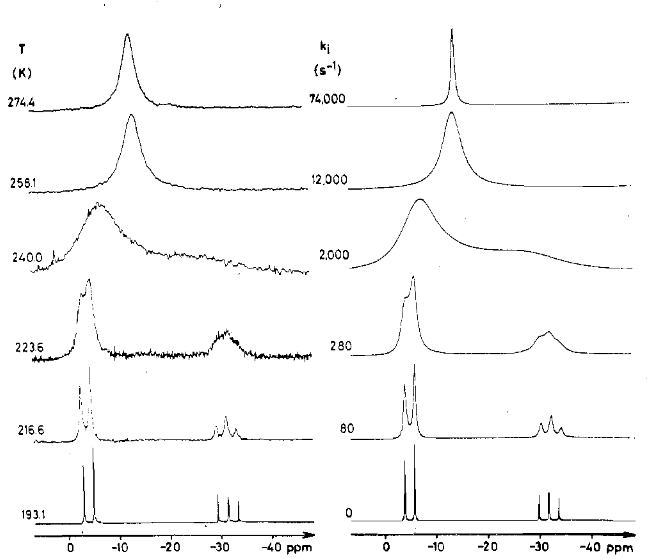

Figure 7. Experimental and calculated $^{31}P\{^1H\}$ FT NMR spectra for the intramolecular exchange of L in $NiBr_2L_3$ ($L = PMe_3$) as a function of temperature in CH_2Cl_2–CD_2Cl_2 (1:1), $[NiBr_2(PMe_3)_3]$ = 0.03 M.

similar behavior was observed by Grimes and Pearson[6b] in the ^1H NMR spectra of $NiX_2(PPhMe_2)_3$ (X = Cl or Br) when the neutral ligand exchange process was studied. They explained this behavior by a rapid square-planar–tetrahedral isomerization of the four-coordinate reaction intermediate. Although this isomerization process is well established for (di- and triarylphosphine)nickel(II) complexes,[28] it was not expected for aryldialkylphosphines and even less for trialkylphosphines. As we detected no bulk paramagnetism in solution by Evans' method[29] and none of the electronic transitions expected from a triplet ground state, the fraction of the paramagnetic species has to be very low. Comparison with the variable temperature electronic spectra shows that this broadening and downfield shift begins at a temperature (about 250 K for X = Cl) where the amount of the four-coordinate $NiX_2(PMe_3)_2$ species increases in solution. The square-planar–tetrahedral isomerization of $NiX_2(PMe_3)_2$ is confirmed by ^{31}P NMR. A solution of $NiCl_2(PMe_3)_2$ shows, at 192 K, only a sharp singlet at δ = −20.4, characteristic of the square-planar species. By increasing the temperature, the singlet broadens and shifts downfield showing the exchange with a paramagnetic species tetrahedral[28] or less probably octahedral.[30] As the chemical shift and the concentration of the paramagnetic species are unknown, we are unable to determine the isomerization equilibrium and rate constants. The presence of paramagnetic species in solution is detected at lower temperature for Cl than for Br. For $NiI_2(PMe_3)_3$, at the highest temperature obtainable in dichloromethane (313 K), the signals due to the axial–equatorial intramolecular exchange process are at coalescence and no effects due to the presence of paramagnetic species are observed.

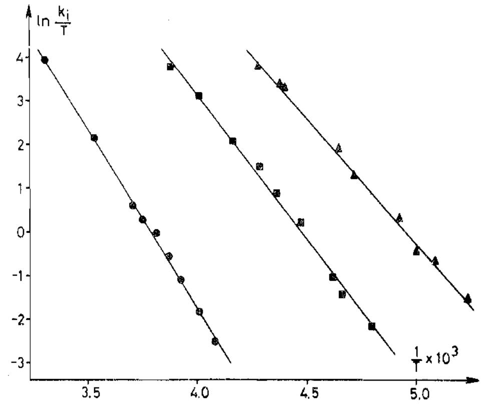

Figure 8. Arrhenius plots for the intramolecular exchange of L in NiX_2L_3 ($L = PMe_3$; X = Cl, Br, or I) in CH_2Cl–CD_2Cl_2 (1:1), $[NiX_2L_3]$ = 0.02 M: ● = I, ■ = Br, ▲ = Cl.

We have determined the activation parameters for mutual exchange of PMe_3 in the complexes $NiX_2(PMe_3)_3$ (X = Cl, Br, or I). The diamagnetic–paramagnetic isomerization and the fact that $NiX_2(PMe_3)_3$ dissociates into $NiX_2(PMe_3)_2$ at high temperature did not allow us to study this exchange at temperatures higher than 250 K for X = Cl and 270 K for X = Br. Results for the three complexes are listed in Table II and Arrhenius-like plots are shown in Figure 8. The rate constants have been obtained as explained in the experimental part. The mutual exchange vector used implied that only one of the two exchanges, E_1 or E_2, occurred at the same time.

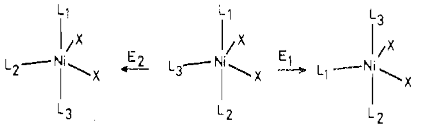

(13)

Examples of calculated and experimental spectra are given in Figure 7 for X = Br. The exchange rate used to obtain the calculated spectra at 274.4 K was obtained by extrapolation of the rates obtained from the line shape analysis at lower temperature. The rates for the mutual PMe_3 exchange decrease in the order Cl > Br > I. This behavior can be explained in terms of nickel–phosphine $d\pi$–$p\pi$ bonding. This bond strength decreases in the order I > Br > Cl, due to parallel decrease of the halide π donation to nickel.[31] $NiI_2(PMe_3)_3$ presents the most covalent Ni–P bond, and the lowest rearrangement rate result which agrees very well with the work of Takats,[32] Osborn,[33] and Caulton.[34] For the mutual exchange in the complexes $NiX_2(PMe_3)_3$ we may consider the following intramolecular rearrangement.

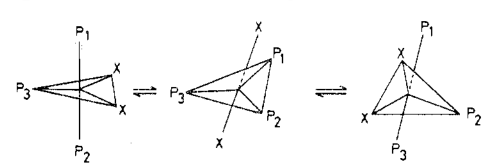

(14)

However, this double Berry pseudorotation would involve an intermediate with two axial halides and until now no such complexes have been reported in the nickel(II)–phosphine chemistry. The positive value (+10.1 to +15.7 cal K^{-1} mol^{-1}) of the activation entropy is closer to those measured for

Table IV. Electronic Spectra of $NiX_2(PMe_3)_n + xPMe_3$ Systems in CH_2Cl_2: $n = 2$ or 3 and x = Free PMe_3/Complex in Molar Ratios 1, 2, and 10 (Concentration of the Solutions about 10^{-2} M)

	$NiX_2(PMe_3)_2$		$NiX_2(PMe_3)_3$		$NiX_2(PMe_3)_3 + PMe_3$		$NiX_2(PMe_3)_3 + 2PMe_3$		$NiX_2(PMe_3)_3 + 10PMe_3$	
X	295 K	180 K	295 K	180 K	295 K	180 K	295 K	180 K	295 K	185 K
Cl			14.8 (380)	15.1 (880)	14.7 (470)	15.1 (700)	14.7 (600)		14.9 (570)	
			17.7 (410)	17.8 (900)	17.4 (510)		17.1 (600)		17.1 (600)	
						18.7 (1690)		18.9 (2250)		18.7 (2010)
	20.8[a] (380)[b]	19.2 (420)	22.2 (250)	23.8 (280)	22.7 (280)	23.8 (455)	23.0 (210)		23.5 (220)	
								26.1		26.3 (200)
Br			14.1 (830)	14.6 (1220)	14.1 (840)		14.1 (900)			
			16.9 (1030)	17.5 (1400)	16.9 (1020)		16.9 (1100)			
	18.2 (1107)	18.1 (1790)				18.7 (2730)		18.7 (2440)	18.3 (1230)	18.8 (2815)
	21.4 (734)	21.7 (1030)	22.7 (290)	23.2 (410)	23.0		23.0 (310)			
								26.3 (370)		26.3 (200)
I			13.8 (1100)	14.0 (1720)	13.5 (1230)		13.5 (1230)		13.5 (1215)	
			16.7 (1870)	17.1 (2650)	16.5 (2200)		16.5 (2220)		16.5 (2110)	
						18.2 (4300)		18.2 (4300)		18.2 (4200)
			18.9 sh	19.0 (1885)						
			23.5 (1680)	23.2 (2300)	24.4 (1600)		24.4 (1630)		24.4 (1590)	
				25.6 (2600)						
					29.0 (3700)	29.4 (2400)	29.0 (3700)	29.4 (2400)		29.4 (2460)

[a] $\nu \times 10^{-3}$, cm^{-1}. [b] ϵ, $M^{-1}\ cm^{-1}$.

dissociative processes ($Ni(CN)_2L_3$, +10.4 to +12.6; $[NiXL_4]^+$, +1.0 to +20;[2] $[Rh(P(OR)_3)_5]^+$, +6.2;[2] $NiH(CN)(PEt_3)_3$, +10.3[35]) than to the values obtained for intramolecular rearrangements without bond breaking[36] ($[Ni(P(OMe)_3)_5]^{2+}$, −0.5; $[Rh(P(OMe)_3)_5]^{2+}$, −5.9). This last evidence and the observed dissociation of $NiX_2(PMe_3)_3$ at ambient temperature allows us to suggest a dissociative pathway for the mutual exchange in these five-coordinate species. The least motion departure of an equatorial ligand with relaxation of the remaining four ligands into a planar geometry will be considered first.

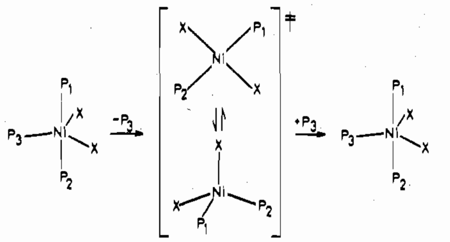

(15a)

This process cannot interchange P_1 or P_2 since it maintains the inequivalence of P_3 from P_1 and P_2. Invoking both planar and tetrahedral species does not solve the problem, since P_1 and P_2 are always symmetry equivalent in both structures. Microscopic reversibility requires that P_3 recombine with any four-coordinate structures with exactly the stereochemistry it used when it departed. This means that P_3 will attack either polyhedron in square brackets to generate always the starting molecule. The interchange requires that P_1 or P_2 is the dissociating phosphine. Thus, whether or not the departure of P_1 causes the four-coordinate fragments to pass through a C_{2v} "tetrahedron" is not evident from the current data so the equilibrium in square brackets is wholly speculative. This latter mechanism (15b) passes through a four-coordinate intermediate which makes previously inequivalent phosphines become equivalent. The significant aspect of this mechanism is that it supports the existence of an axial dissociative reaction for TBP molecules which is an alternative to the "least motion" departure of an equatorial ligand. It should be added that it does not mean that the axial phosphines are more labile than the equatorial one; it means only that the axial–equatorial interchange requires an axial phosphine dissociation. A dissociative process with a halide loss can be excluded since the addition of $[NBu_4]Cl$ to a solution of $NiCl_2L_3$ has no influence on the phosphine interchange rate.

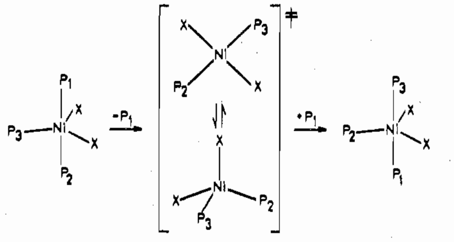

(15b)

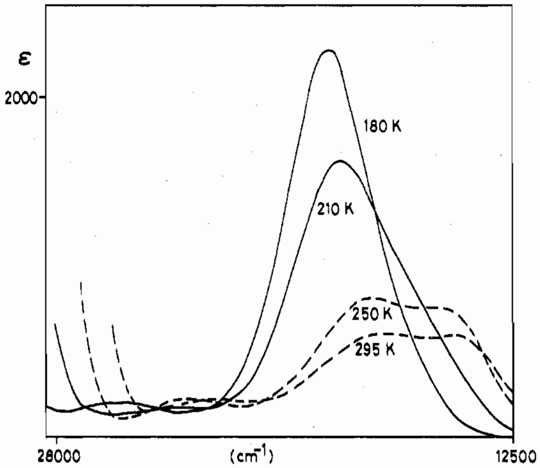

Figure 9. Variable-temperature (180–295 K) electronic spectra of a solution of $NiCl_2(PMe_3)_3$ and PMe_3 in CH_2Cl_2, $[NiCl_2(PMe_3)_3]$ = 0.85×10^{-2} M and $[PMe_3] = 3 \times 10^{-2}$ M.

2.3 $NiX_2(PMe_3)_3$ (X = Cl, Br, or I) Solutions with Excess PMe_3. Addition of PMe_3 to dichloromethane solutions of $NiX_2(PMe_3)_3$ (X = Cl, Br, or I) leads at room temperature to the stabilization of the five-coordinate $NiX_2(PMe_3)_3$, according to eq 1 (Figure 5). The effect of lowering the temperature of a solution of $NiCl_2(PMe_3)_3$ (10^{-2} M) with an excess of PMe_3 (2×10^{-2} M) is shown in Figure 9. A tremendous variation of the electronic spectrum, in shape and intensity, is observed, indicating the formation, at low temperature, of a new chemical species. Similar spectra are obtained for $NiBr_2(PMe_3)_3$ and $NiI_2(PMe_3)_3$ (Table IV). The temperature effect is reversible. By increasing the amount of excess PMe_3 (PMe_3/complex = 2 to 10 molar ratio), no modification of the low-temperature spectrum occurs and only the temperature range, where the low-temperature species is stabilized, is observed to increase with the ratio PMe_3/complex. As shown by the increase of conductivity of the solution when the temperature is lowered, the $[NiX(PMe_3)_4]X$ species must be formed according to eq 2.

The ^{31}P NMR spectra of solutions with an excess of PMe_3 show, at 173 K, a sharp singlet at −14.6 ppm for X = Cl, at −15.7 ppm for X = Br, and at −18.4 ppm for X = I. When the ratio $PMe_3/NiX_2(PMe_3)_3 > 1$, the only new resonance observed is that of free PMe_3 at 61.2 ppm. This pattern may be relevant either to a species with four equivalent phosphorus ligands or to a fast intramolecular exchange process of nonequivalent ligands still operating at 173 K. The presence of a very fast intramolecular phosphorus exchange is confirmed since at 114 K in chlorodifluoromethane the ligand exchange is almost frozen on the NMR time scale for X = Cl and the ^{31}P NMR spectrum consists then of two triplets (Table III). The electronic spectrum of $[NiCl(PMe_3)_4]Cl$ has been determined in the same conditions (in $CHClF_2$ solutions at 114 K). It is similar to the one previously obtained at 180 K (in CH_2Cl_2), indicating that the same species is present at 114 and 180 K. The ^{31}P NMR spectrum of $[NiCl(PMe_3)_4]Cl$ is the same as that of $[NiCl(PMe_3)_4]BF_4$ (Table III). The latter has been characterized as a low-spin, five-coordinate Ni(II) complex of trigonal-bipyramidal geometry with Cl in equatorial position.[9] Thus this leads us to propose a trigonal-bipyramidal structure for the $[NiCl(PMe_3)_4]Cl$ species in CH_2Cl_2 and $CHClF_2$ solutions.

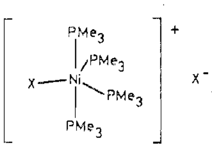

For $[NiX(PMe_3)_4]X$ (X = Br or I) solutions in $CHClF_2$, the ^{31}P NMR spectra at 114 K are broad singlets showing that the intramolecular PMe_3 exchange is still not frozen but the rate of this exchange is higher for X = I than for X = Br ($W_{1/2}$ = 8 Hz for X = I and $W_{1/2}$ = 25 Hz for X = Br). Thus the rates of intramolecular exchange in the $[NiX(PMe_3)_4]X$ complexes are in the order I > Br > Cl, that is, the reverse of the order observed in $[NiX(PMe_3)_4]BF_4$ compounds.[9] For the latter compound, the slow exchange limit spectra consisting of two triplets are observed at higher temperature (140 K and above). This shows that the rate of the intramolecular phosphorus exchange is faster in the case of X^- than in the case of BF_4^- as counterion. In $[NiX(PMe_3)_4]BF_4$ a Berry pseudorotation mechanism was proposed for the intramolecular phosphorus exchange. The faster exchange rates observed in $[NiX(PMe_3)_4]X$ can be reasonably related to the nucleophilic attack of the complex by the halide ion. As iodide is the best nucleophile, the order of the rate constants (I > Br > Cl) observed for the three complexes can be explained. In order to prove this nucleophilic attack, we have determined the effect of adding variable amounts of bromine to the $[NiBr(PMe_3)_4]BF_4$ complex. We have found a second-order rate law for the intramolecular exchange of PMe_3: first order in bromine and first order in complex. This rate law confirms the participation of the ionized halide in the transition state. The following mechanism may be considered.

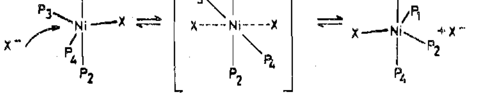

(16)

The outer-sphere halide ion attacks the nickel center trans to the equatorial halide to form a 20-electron transition state. A 20-electron transition state has never been reported, to our knowledge, in d^8 chemistry. Recently, Hynes and Brannick[37] reported a ligand-exchange reaction in a high-spin 18-electron five-coordinate Ni(II) complex occurring through an associative mechanism, showing that for high-spin species, Tolman's rule[38] does not apply. However, for low-spin Ni(II) complexes, until now, only dissociative ligand-exchange mechanisms have been reported.[6b,7] The mechanism proposed above involves a concerted halide bond-making and bond-breaking process. As indicated by the increase of the reaction rates with the halide nucleophilicity, we are dealing with an associative activation mode. Therefore we must consider an associative interchange mechanism I_a for these low-spin five-coordinate Ni(II) 18-electron complexes.

Addition of an excess of PMe_3 to solutions of $[NiX(PMe_3)_4]X$ gives rise to two singlets in the ^{31}P NMR spectra at 173 K, due to $[NiX(PMe_3)_4]X$ and free PMe_3, and no change is observed in the electronic spectra. Even the addition of very large amounts of PMe_3 does not lead to a halide displacement to obtain $[Ni(PMe_3)_5]X_2$. This last cation has been prepared in $CHClF_2$ by adding PMe_3 to $[Ni(PMe_3)_4](BF_4)_2$. The ^{31}P NMR spectra of such a solution show two singlets at 170 K, due to the phosphine and to the new $[Ni(PMe_3)_5]^{2+}$ species in fast intramolecular exchange. By lowering the temperature to 114 K this last singlet splits into a triplet and a quadruplet (Table III) characteristic of a five-coordinate trigonal-bipyramidal structure. The free energy of activation for the intramolecular phosphine exchange has been determined at one temperature by the method described for $NiX_2(PMe_3)_3$, using a suitable exchange vector. The value obtained ($\Delta G^* = 6.2 \pm 0.2$ kcal/mol at 130 K) is smaller than those obtained for the similar exchange in $[NiX(PMe_3)_4]BF_4$ species (Table II). We therefore conclude, in this case too, to a Berry pseudorotation.

Solutions containing $[NiX(PMe_3)_4]X$ and free PMe_3 provide a good opportunity to investigate the following intermolecular exchange.

$$[NiX(PMe_3)_4]X + {}^*PMe_3 \rightleftharpoons [NiX(PMe_3)_3({}^*PMe_3)]X + PMe_3 \quad (17)$$

With the rate of intramolecular PMe_3 exchange in $[NiX(PMe_3)_4]X$ being very high at 173 K and above, the intermolecular PMe_3 exchange process can be considered as a single two-site exchange. A similar approach was used by English, Meakin, and Jesson, when determining the rate of ligand dissociation in the $[HNi(PEt_3)_4]^+$ species.[2] However, the study is complicated by the temperature dependence of the stability of the $[NiX(PMe_3)_4]X$ species. When the temperature is increased, K_{cat} decreases and thus appreciable amounts of $NiX_2(PMe_3)_3$ and $NiX_2(PMe_3)_2$ are formed, causing, as expected, a broadening and a downfield shift of the collapsed lines. We therefore have determined the exchange rate for X = Cl and X = Br at a low enough temperature. The activation parameters (Table II) for the intermolecular ligand exchange are determined by the method described in the experimental part. The rate law is first order in complex and zero order in PMe_3. For both chloride and bromide complexes, the activation entropies of the intermolecular exchange process are positive. Therefore, we propose a dissociative D mechanism with the planar $[NiX(PMe_3)_3]^+$ species as intermediate. The $[NiX(PMe_3)_3]BF_4$ (X = Cl or Br) complexes have been isolated[39] and their NMR data are given in Table III. The activation step for this ligand-exchange reaction (dissociation of phosphine) is the same as that used previously to explain the intramolecular PMe_3 exchange in the $NiX_2(PMe_3)_3$ complexes. We again observe an increase of the rates in the order I < Br < Cl; moreover, the activation parameters are very similar for both processes.

Conclusion

As shown by ^{31}P NMR and electronic spectroscopies, the following solution equilibria (in CH_2Cl_2 or $CHClF_2$) take place in the NiX_2–PMe_3 system between 113 and 295 K.

$$\text{SP-NiX}_2(\text{PMe}_3)_2 \rightleftharpoons \text{T-NiX}_2(\text{PMe}_3)_2 \quad \text{X = halide} \qquad (18)$$

$$\text{NiX}_2(\text{PMe}_3)_2 + \text{PMe}_3 \rightleftharpoons \text{NiX}_2(\text{PMe}_3)_3 \quad \text{X = CN, halide} \qquad (19)$$

$$\text{NiX}_2(\text{PMe}_3)_3 + \text{PMe}_3 \rightleftharpoons [\text{NiX}(\text{PMe}_3)_4]\text{X} \quad \text{X = halide} \qquad (20)$$

$$[\text{NiX}(\text{PMe}_3)_3]\text{BF}_4 + \text{PMe}_3 \rightleftharpoons [\text{NiX}(\text{PMe}_3)_4]\text{BF}_4 \quad \text{X = halide} \qquad (21)$$

$$[\text{Ni}(\text{PMe}_3)_4](\text{BF}_4)_2 + \text{PMe}_3 \rightleftharpoons [\text{Ni}(\text{PMe}_3)_5](\text{BF}_4)_2 \qquad (22)$$

The following four-coordinate species have been characterized: $NiX_2(PMe_3)_2$ (X = CN, Cl, or Br) and $[NiX(PMe_3)_3]^+$ (X = Cl or Br). On the whole temperature range, the main species is the square-planar (SP) isomer. However, a partial isomerization toward a tetrahedral (T) paramagnetic species is proposed for $NiX_2(PMe_3)_3$ when X = Cl or Br.

Three five-coordinate species have been identified: $NiX_2(PMe_3)_3$ (X = CN, Cl, Br, or I), $[NiX(PMe_3)_4]^+$ (X = Cl, Br, or I), and $[Ni(PMe_3)_5]^{2+}$. These complexes present a trigonal-bipyramidal geometry with the halide(s) in equatorial position and the cyanides in axial position. This is consistent with the fact that, until now, no structure with a halide in axial position has been reported in nickel(II)–phosphine chemistry. These five-coordinate complexes are stereochemically nonrigid. They undergo both fast intra- and intermolecular phosphine exchange processes, these processes following various pathways.

The *intramolecular phosphine exchanges* are characterized by small free energies of activation ΔG^*. The value for $[Ni(PMe_3)_5](BF_4)_2$ is 6.2 ± 0.2 kcal mol^{-1} at 130 K and is consistent with a Berry pseudorotation. In $[NiX(PMe_3)_4]^+$ the intramolecular exchange occurs through two different processes, depending on the counterion. When the counterion is BF_4^-, the measured ΔG^*'s (at 169 K, 6.6 for Cl, 7.8 for Br, and 8.2 kcal mol^{-1} for I) agree with a Berry pseudorotation with the nickel–halide bond as pivot. However, when the counterion is a halide the barrier for the phosphine exchange is considerably lowered. The ΔG^*'s sequence is now reversed, the values decreasing with increasing nucleophilicity of the counterion. Moreover, the phosphine exchange rate is now proportional to the ionic halide concentration. The proposed mechanism is an associative interchange I_a process, involving a nucleophilic attack by an ionic halide, followed by the formation of a 20-electron transition state. In $NiX_2(PMe_3)_3$ the energy barriers for the axial–equatorial phosphine exchange are higher (at 230 K, 9.2–13.0 kcal mol^{-1}) than those encountered in the former species. In this case, we propose a dissociative D mechanism, involving loss of an axial phosphine to form a four-coordinate intermediate.

The *intermolecular phosphine exchanges* between $Ni(CN)_2(PMe_3)_3$ and free PMe_3 occur through a dissociative mechanism D. The free energy of the intermediate, the square-planar $Ni(CN)_2(PMe_3)_2$, is only 4.9 kcal mol^{-1} higher than that of the five-coordinate reactant at 298 K. The PMe_3 intermolecular exchange reaction on $NiX_2(PMe_3)_3$ could not be studied, as these complexes react quantitatively with PMe_3 to form $[NiX(PMe_3)_4]X$. The PMe_3 exchange on these latter complexes follows a D mechanism, with $[NiX(PMe_3)_3]^+$ as intermediate. The exchange rate is faster when X is a chlorine than when X is a bromine.

The five-coordinate nickel(II)–phosphine complexes exhibit a great variety of phosphine-exchange mechanisms, the nature of the ligand playing an important role in the mechanism. For example, $[NiL_5]^{2+}$, $[NiXL_4]Y$, and NiX_2L_3 are all trigonal-bipyramidal, stereochemically nonrigid complexes, but the intramolecular phosphine exchange in these species occurs through different mechanisms: a Berry pseudorotation in $[NiL_5]^{2+}$ and $[NiXL_4]BF_4$, a tetrahedral jump in $[NiHL_4]^+$,[2] a dissociative D mechanism in NiX_2L_3, and an associative interchange I_a in $[NiX(PMe_3)_4]X$. These results predict different reactivities for the various complexes when they will be involved in organometallic and catalytic reactions.

Acknowledgment. We thank P. Meakin for making available his computer program PZDMCS and K. G. Caulton for suggesting mechanism 15b. This work was supported by the Swiss National Science Foundation under Grant No. 2.921-0.77.

Registry No. $Ni(CN)_2(PMe_3)_2$, 38889-86-0; $NiCl_2(PMe_3)_2$, 20087-67-6; $NiBr_2(PMe_3)_2$, 38907-48-1; $Ni(CN)_2(PMe_3)_3$, 54515-54-7; $NiCl_2(PMe_3)_3$, 53177-14-3; $NiBr_2(PMe_3)_3$, 53188-33-3; $NiI_2(PMe_3)_3$, 53188-34-4; $[NiCl(PMe_3)_4]Cl$, 68707-98-2; $[NiCl(PMe_3)_4]BF_4$, 67889-84-3; $[NiBr(PMe_3)_4]Br$, 68707-99-3; $[NiBr(PMe_3)_4]BF_4$, 67889-86-5; $[NiI(PMe_3)_4]I$, 68708-00-9; $[NiI(PMe_3)_4]BF_4$, 67889-82-1; $[Ni(PMe_3)_5](BF_4)_2$, 68708-02-1.

Supplementary Material Available: Kinetic data (5 pages). Ordering information is given on any current masthead page.

References and Notes

(1) (a) Université de Lausanne. (b) Based, in part, on the Ph.D. Thesis of P.F.M., Université de Lausanne. (c) Laboratorie de Chimie de Coordination.

(2) A. D. English, P. Meakin, and J. P. Jesson, *J. Am. Chem. Soc.*, **98**, 422 and 7590 (1976), and references therein.

(3) P. R. Hoffman and K. G. Caulton, *J. Am. Chem. Soc.*, **97**, 4221 (1975).

(4) K. A. Jensen and O. Dahl, *Acta Chem. Scand.*, **22**, 1044 (1968); O. Dahl, *ibid.*, **23**, 2342 (1969); A. Merle, M. Dartiguenave, Y. Dartiguenave, J. W. Dawson, and H. B. Gray, *J. Coord. Chem.*, **3**, 199 (1974); A. Merle, M. Dartiguenave, and Y. Dartiguenave, *J. Mol. Struct.*, **13**, 413 (1972).

(5) P. Meier, A. E. Merbach, M. Dartiguenave, and Y. Dartiguenave, *J. Am. Chem. Soc.*, **98**, 6402 (1976), and this work.

(6) (a) E. J. Lukosius and K. J. Coskran, *Inorg. Chem.*, **14**, 1922, 1926 (1975). (b) C. G. Grimes and R. G. Pearson, *Inorg. Chem.*, **13**, 970 (1974).

(7) B. B. Chastain, D. W. Meek, E. Billig, J. E. Hix, Jr., and H. B. Gray, *Inorg. Chem.*, **7**, 2412 (1968).

(8) J. W. Dawson, T. J. McLennan, W. Robinson, A. Merle, M. Dartiguenave, Y. Dartiguenave, and H. B. Gray, *J. Am. Chem. Soc.*, **96**, 4428 (1974).

(9) M. Dartiguenave, Y. Dartiguenave, C. Saint-Joly, A. Gleizes, J. Galy, P. Meier, and A. Merbach, *Inorg. Chem.*, **17**, 3503 (1978).

(10) W. Wolfsberger and H. Schmidbauer, *Synth. Inorg. Met.-Org. Chem.*, **4**, 149 (1974).

(11) C. Ammann, P. Meier, and A. E. Merbach, submitted for publication.

(12) H. M. McConnell, *J. Chem. Phys.*, **28**, 430 (1958).

(13) P. Meakin and J. P. Jesson, *J. Am. Chem. Soc.*, **95**, 7272 (1973).

(14) R. Morassi, I. Bertini, and L. Sacconi, *Coord. Chem. Rev.*, **11**, 343 (1973).

(15) K. N. Raymond, P. W. R. Corfield, and J. A. Ibers, *Inorg. Chem.*, **7**, 1362 (1968).

(16) H. M. Powell, D. J. Watkins, and J. B. Wilford, *J. Chem. Soc. A*, 1803 (1971). D. W. Allen, I. T. Millar, and F. G. Mann, *J. Chem. Soc. A*, 1101 (1969).

(17) E. L. Muetterties and L. J. Guggenberger, *J. Am. Chem. Soc.*, **96**, 1748 (1974). J. K. Kouba and S. S. Wreford, *Inorg. Chem.*, **15**, 1463 (1976).

(18) E. L. Muetterties and R. A. Schunn, *Q. Rev., Chem. Soc.*, **20**, 245 (1966).

(19) J. K. Stalick and J. A. Ibers, *Inorg. Chem.*, **9**, 453 (1970).

(20) J. K. Stalick and J. A. Ibers, *Inorg. Chem.*, **8**, 1084, 1090 (1969).

(21) P. Rigo, G. Guastalla, and A. Turco, *Inorg. Chem.*, **8**, 375 (1969). P. Rigo, C. Pecile, and A. Turco, *Inorg. Chem.*, **6**, 1636 (1967).

(22) E. C. Alyea and D. W. Meek, *J. Am. Chem. Soc.*, **91**, 5761 (1969).

(23) R. G. Hayter, *Inorg. Chem.*, **2**, 933 (1963). J. A. Bertrand and D. L. Plymale, *Inorg. Chem.*, **5**, 879 (1965).

(24) P. Rigo and M. Bressan, *Inorg. Chem.*, **11**, 1314 (1972).

(25) K. J. Coskran, J. M. Jenkins, and J. G. Verkade, *J. Am. Chem. Soc.*, **90**, 5437 (1968).

(26) L. J. VandeGriend, J. C. Clardy, and J. G. Verkade, *Inorg. Chem.*, **14**, 711 (1975).

(27) D. S. Milbrath, J. P. Springer, J. C. Clardy, and J. G. Verkade, *Inorg. Chem.*, **14**, 2665 (1975).

(28) L. H. Pignolet and W. DeW. Horrocks, Jr., *J. Am. Chem. Soc.*, **91**, 3976 (1969). L. H. Pignolet, W. DeW. Horrocks, Jr., and R. H. Holm, *J. Am. Chem. Soc.*, **92**, 1855 (1970). G. N. LaMar and E. O. Sherman, *J. Am. Chem. Soc.*, **92**, 2691 (1970). M. C. Browning, J. R. Mellor, D. J. Morgan, S. A. J. Pratt, L. E. Sutton, and L. M. Venanzi, *J. Chem. Soc.*, 693 (1962).

(29) D. F. Evans, *J. Chem. Soc.*, 2003 (1959).

(30) K. Cheng and B. M. Foxman, *J. Am. Chem. Soc.*, **99**, 8102 (1977).

(31) E. A. LaLancette and D. R. Eaton, *J. Am. Chem. Soc.*, **86**, 5145 (1964).

(32) L. Kruczynski, L. K. K. LiShingMan, and J. Takats, *J. Am. Chem. Soc.*, **96**, 4006 (1974).

(33) S. T. Wilson, N. J. Coville, J. R. Shapely, and J. A. Osborn, *J. Am. Chem. Soc.*, **96**, 4038 (1974).

(34) J. S. Miller and K. G. Caulton, *J. Am. Chem. Soc.*, **97**, 1067 (1975).
(35) J. D. Druliner, A. D. English, J. P. Jesson, P. Meakin, and C. A. Tolman, *J. Am. Chem. Soc.*, **98**, 2156 (1976).
(36) J. P. Jesson and P. Meakin, *J. Am. Chem. Soc.*, **96**, 5760 (1974); **95**, 7272 (1973).
(37) M. J. Hynes and P. F. Brannick, *J. Chem. Soc., Chem. Commun.*, 942 (1977).
(38) C. A. Tolman, *Chem. Soc. Rev.*, **1**, 337 (1972).
(39) P. F. Meier, A. E. Merbach, M. Dartiguenave, and Y. Dartiguenave, to be submitted for publication.

Contribution from the Department of Chemistry,
The University of North Carolina, Chapel Hill, North Carolina 27514

Ligand-Bridged Complexes of Ruthenium(III). Magnetic Properties of Ligand-Bridged, Dimeric and Pyrazine-Bridged, Polymeric Complexes

EUGENE C. JOHNSON, ROBERT W. CALLAHAN, RICHARD P. ECKBERG, WILLIAM E. HATFIELD,*
and THOMAS J. MEYER*

Received March 17, 1978

A series of ligand-bridged complexes of ruthenium(III) have been prepared utilizing pyrazine, 4,4′-bipyridine, and 1,2-bis(4-pyridyl)ethane as the bridging ligands. The preparations involve the use of Ce(IV) to oxidize complexes of ruthenium(II) whose preparations were described previously. Dimeric complexes of the three bridging ligands, as well as trimeric and tetrameric pyrazine-bridged complexes, were prepared. The electronic spectra and magnetic properties of these formally low-spin d^5 metal complexes were studied, the latter down to liquid-helium temperatures. The flexibility in the synthetic chemistry allowed, in principle, for a systematic study of the magnetic effects of different metal–metal interactions arising from changes in the bridging ligand and in polymer chain length. However, the magnetic results indicate little, if any, interactions in any of the complexes including the polymeric cases where the possibility of extended metal–metal interactions exists.

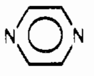
pyrazine

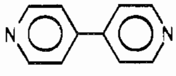
4,4′-bipyridine

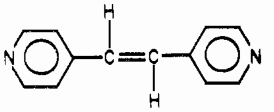
trans-1,2-bis(4-pyridyl)ethylene

In past work we have developed a synthetic chemistry which has led to the preparation of a series of ligand-bridged dimeric and oligomeric complexes of ruthenium.[1] Dimeric complexes have been prepared using a series of N-heterocyclic ligands, (bpy)$_2$ClRu(L)RuCl(bpy)$_2^{2+}$ (bpy is 2,2′-bipyridine; L is pyrazine (pyz), 4,4′-bipyridine (4,4′-bpy), or *trans*-1,2-bis(4-pyridyl)ethylene (BPE)), and pyrazine-bridged oligomeric complexes have been prepared with controlled chain lengths, [(bpy)$_2$ClRu(pyz)[Ru(bpy)$_2$(pyz)]$_n$RuCl(bpy)$_2$]$^{(2n+2)+}$ (n = 0–4). The preparative chemistry involved uses the reactivity properties of the bound nitrosyl and nitro groups in a series of stepwise reactions.[2] From the known stereochemistry of bis(2,2′-bipyridine) complexes, the coordination geometry at each ruthenium site in the oligomeric chains is most likely cis.[3]

Questions of fundamental interest in ligand-bridged metal complexes are the nature and extent of metal–metal interactions across the bridging ligands and the effects of the interactions on the chemical and physical properties of the system. The role of metal–metal interactions has been studied extensively in dimeric ruthenium complexes especially in mixed-valence systems.[4,5] From these studies it has been shown that the extent of electronic interaction can vary from interactions which are sufficiently strong to modify the chemical and physical properties of the system in a significant way[6–8] to weak interactions where the separate redox sites are only slightly perturbed compared to isolated monomeric sites.[4,5,9–11] The differences in properties observed appear to be understandable based on the properties of a series of closely related dimeric compounds.[4b,11]

Localized valences are favored for cases where significant vibrational trapping energies exist for the excess electron. The trapping energy arises because a change in oxidation state at the metal leads to differences in the inner- and the outer-coordination spheres at the two redox sites. Orbital overlap leads to electronic delocalization and reduces the vibrational trapping energy by making the two sites more nearly equivalent. In one limit, the electronic resonance energy arising from the overlap is sufficient to overcome the trapping energy, and the vibrational structures at the two sites become identical. Delocalization is favored by strong metal–metal overlap, and in ligand-bridged systems, the distance for significant overlap can be extended by mixing metal orbitals with orbitals on the bridging ligand.

Ruthenium(III) is a readily accessible oxidation state in dimeric 2,2′-bipyridine complexes of ruthenium as shown by electrochemical studies on ions like [(bpy)$_2$ClRu(pyz)RuCl(bpy)$_2$]$^{2+}$.[9,10] Complexes of ruthenium(III) have been found to be spin-paired d^5 cases with one unpaired electron[12–14] which means that in dimeric ions like the 4+ ion, [(bpy)$_2$ClRu(pyz)RuCl(bpy)$_2$]$^{4+}$ magnetic techniques provide a sensitive probe for detecting Ru(III)–Ru(III) electronic interactions. Magnetic measurements on ligand-bridged, oligomeric complexes containing ruthenium in the 3+ oxidation state could reveal extended magnetic interactions involving more than two metal sites. It is conceivable that cooperative interactions within such polymeric chains could lead to materials having chemical and electronic properties intermediate between the properties of simple dimers and the properties of extensively linked, solid-state materials.

Experimental Section[15]

Measurements. Infrared spectra were recorded on a Perkin-Elmer 421 spectrophotometer in KBr pellets at room temperature. Ultraviolet–visible spectra were recorded on Cary Model 14, Cary Model 17, or Unicam Model SP800B spectrophotometers in 1-cm silica cells using MCB Spectrograde acetonitrile at room temperature. ESCA measurements were obtained on a Du Pont Instruments 650 electron spectrometer equipped with a Du Pont Instruments multichannel analyzer. Samples were prepared by grinding the solid complex into the surface of a gold sample probe using a clean glass rod. Magnetic susceptibility measurements from 1.7 to 77 K were conducted on powdered samples of the complexes using a PAR Foner-type vibrating

0020-1669/79/1318-0618$01.00/0 © 1979 American Chemical Society